Magnetic and magnetotransport properties in Cu and Fe co-doped bulk In_2O_3 and ITO

2008 J. Phys.: Condens. Matter 20 475204

(http://iopscience.iop.org/0953-8984/20/47/475204)

IOP PUBLISHING JOURNAL OF PHYSICS: CONDENSED MATTER

J. Phys.: Condens. Matter **20** (2008) 475204 (6pp) doi:10.1088/0953-8984/20/47/475204

Magnetic and magnetotransport properties in Cu and Fe co-doped bulk In_2O_3 and ITO

H W Ho, B C Zhao, B Xia, S L Huang, Y Wu, J G Tao, A C H Huan and L Wang[1]

Division of Physics and Applied Physics, School of Physical and Mathematical Sciences, Nanyang Technological University, 21 Nanyang Link, 637371, Singapore

E-mail: wanglan@ntu.edu.sg

Received 8 July 2008, in final form 6 October 2008
Published 29 October 2008
Online at stacks.iop.org/JPhysCM/20/475204

Abstract

A systematic study of structural, magnetic, and transport properties was performed on $(In_{0.85-x}Fe_{0.15}Cu_x)_2O_3$ (IFCO) and $(In_{0.80-x}Sn_{0.05}Fe_{0.15}Cu_x)_2O_3$ (ISFCO) compounds with $x = 0$, 0.02, and 0.05. All the studied samples show clear room temperature ferromagnetism and the saturated magnetic moment decreases monotonically with increasing Cu-doping content. Detailed analysis based on the magnetic measurement rules out the ferromagnetism due to Fe_3O_4 and $CuFe_2O_4$ impurities. A crossover from semiconducting to metallic transport behavior is observed in IFCO samples, whereas only semiconducting behavior is detected in ISFCO. Low temperature resistivity decreases monotonically with increasing Cu-doping level due to the increasing electron concentration. Positive magnetoresistance is observed in IFCO, which also shows an anomalous Hall effect at 5 and 300 K. No magnetoresistance or AHE is found in ISFCO compounds. All the electric transport measurement results can be clarified by a two-channel transport model.

1. Introduction

Diluted magnetic semiconductors (DMSs) have attracted much attention for their potential applications in spintronics [1]. Following the theoretical prediction by Dietl *et al* of room temperature ferromagnetism (FM) in ZnO-based DMSs [2], many 3d-transition-metal-doped wide-band-gap oxide semiconductors have been investigated. Room temperature FM has been reported in transition-metal-doped ZnO, TiO_2, SnO_2, and In_2O_3 [3–10]. However, the intrinsic origin of ferromagnetism in these systems remains controversial [11, 12]. This awkward condition is mainly due to the weakness of the magnetization of DMS samples. The presence of very small amounts of impurity phases can generate a magnetization higher than the intrinsic magnetization of the DMS sample.

In_2O_3 is a transparent wide-band-gap (3.75 eV) semiconductor [13]. It crystallizes in the cubic bixbyite structure with a lattice parameter $a = 10.12$ Å and can be prepared as an n-type semiconductor with a high electrical conductivity by introducing oxygen deficiencies or by Sn doping (ITO) [14]. Because of the high solubility of Fe in In_2O_3 (>20%), homogeneous solid solution can be realized at least up to 15% Fe doping according to recent literature [14, 15], which makes the material a good system to study the basic physics of DMS. The existence of very small amounts of impurity phases will no longer be a problem if the Fe in the cubic bixbyite can realize ferromagnetism, because the intrinsic ferromagnetic signal will be much larger than that from the impurity phases. The magnetic state of Fe-doped In_2O_3 is determined by the synthesis methods. Several magnetic states such as paramagnetic [12], spin-glass [16], and ferromagnetic have been observed in Fe-doped In_2O_3 [14, 17]. In order to achieve multiple valence in the sample, Cu was co-doped with Fe into In_2O_3 and clear room temperature FM can appear in these samples [14, 15]. FM was also observed in Fe-doped ITO thin film, where ferromagnetism is suggested to originate from nanosized Fe clusters in the highest oxidation state Fe_2O_3 [18]. Recent magnetic measurements, HRTEM, XANES, EXAFS and XAS results

[1] Author to whom any correspondence should be addressed.

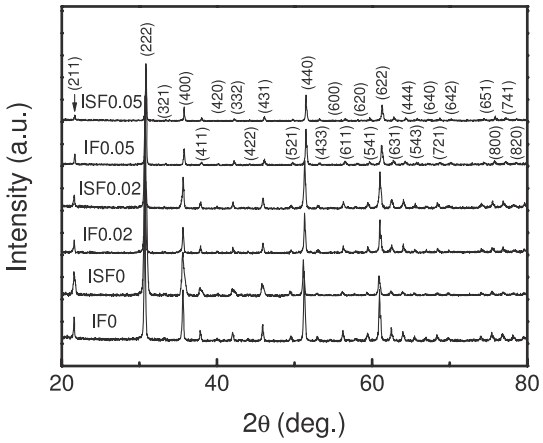

Figure 1. X-ray diffraction patterns for IFCO and ISFCO bulk samples. In the figure, IFCO and ISFCO samples are abbreviated as IF0, 0.02, 0.05 and ISF0, 0.02, 0.05, respectively.

indicate the intrinsic ferromagnetism can be realize in Fe-doped and Cu–Fe co-doped In_2O_3 with certain synthesis methods [14, 17, 19].

In order to study the charge-doping effect, such as Cu and Sn doping, we fixed Fe concentration at 15% and performed a comparison study for the evolution of the magnetization, MR, and Hall effects with increasing Cu-doping level in both In_2O_3 and ITO bulk polycrystalline samples. All studied samples show clear room temperature FM. Our detailed magnetic analysis proves that the FM is not due to the Fe_3O_4 and $CuFe_2O_4$ impurities. The FM is determined by the interaction between the randomly distributed Fe in the bixbyite In_2O_3 structure. Obvious AHE and large positive MR at low temperatures were observed in the doped In_2O_3 but not in the doped ITO samples. All the electrical transport data can be clarified by a proposed two-channel transport model.

2. Experimental considerations

$(In_{0.85-x}Fe_{0.15}Cu_x)_2O_3$ (IFCO) and $(In_{0.80-x}Sn_{0.05}Fe_{0.15}Cu_x)_2O_3$ (ISFCO) bulk samples with $x = 0$, 0.02, and 0.05 were prepared by the conventional solid state reaction method. Stoichiometric precursor powders In_2O_3, SnO_2, Fe_2O_3, and CuO were weighed and mixed in stoichiometric ratios. The mixed powders were then sintered in air at 900 and 1000 °C for 24 h with intermediate grinding. Finally, the reacted materials were reground, pressed into small pellets, and sintered at 1100 °C for 24 h in air or vacuum ($\sim 10^{-2}$ Torr).

The structure of the samples was characterized by means of x-ray diffraction (XRD) using Cu Kα radiation at room temperature. The magnetotransport measurements were performed on a Quantum Design physical properties measurement system (PPMS). The Van der Pauw method was used to measure the resistivity. The standard four-probe method was employed for Hall measurement. The magnetic measurements were carried out with a vibrating sample magnetometer (VSM) attached to the PPMS system in the temperature range of 5–320 K.

Table 1. Structural, magnetic and transport parameters of IFCO and ISFCO samples. M_S, n, and μ are the saturated magnetic moment, electron concentration, and electron mobility, respectively.

			M_S (μ_B/Fe)		n (10^{18} cm^{-3})		μ (cm^2 V^{-1} s^{-1})	
	x	d (Å)	5 K	300 K	5 K	300 K	5 K	300 K
IFCO	0	10.093	0.868	0.838	4.59	3.60	11.98	20.4
	0.02	10.089	0.864	0.797	2.38	3.09	19.7	32.1
	0.05	10.082	0.581	0.502	3.37	3.99	10.5	23.7
ISFCO	0	10.087	0.353	0.291	27.2	23.8	4.51	7.95
	0.02	10.081	0.347	0.243	54.1	56.7	10.5	13.1
	0.05	10.076	0.193	0.132	62.8	73.5	9.95	10.4

3. Results and discussion

The XRD patterns show the phase difference between the samples sintered in air and vacuum. An obvious impurity phase peak such as SnO_2 can be observed in the XRD patterns for the sample sintered in air and disappears when sintering in vacuum. Figure 1 shows the XRD patterns for all the studied samples sintered in vacuum. The diffraction peaks in the figure are consistent with the standard pattern of cubic In_2O_3; no obvious impurity phase (such as Fe_3O_4, Fe_2O_3, or $CuFe_2O_4$) was detected. Considering the 15% Fe doping and the detection limit ($\sim$1% impurity phase) of our XRD facility, we can conclude that most of the Fe replaces In and form cubic bixbyite structure $(In_{0.85-x}Fe_{0.15}Cu_x)_2O_3$ and $(In_{0.80-x}Sn_{0.05}Fe_{0.15}Cu_x)_2O_3$. This result is consistent with the large solubility limit (>20%) of Fe in In_2O_3 as shown in previous literature. A shift of XRD peak positions related to lattice constant changes was clearly observed when the concentration of Cu was varied. The lattice constant d obtained from the XRD patterns is shown in table 1, which decreases monotonically with increasing Cu-doping content, suggesting the incorporation of Cu ions into the cubic lattice of In_2O_3. The result is consistent with the fact that the Cu^{2+}/Cu^{3+} ion is smaller than the In^{3+}. From the XRD results, we cannot exclude the existence and the magnetic contribution of magnetic impurity phases (Fe_3O_4, Fe_2O_3 and $CuFe_2O_4$). However, it is obvious that most of the Fe and Cu dissolve into the In_2O_3 cubic bixbyite structure. It should be noted that the chemical homogeneity does not guarantee magnetic homogeneity in ferromagnetic materials. It is well known that many chemically homogeneous manganites and cobaltites show magnetoelectric phase separation [29, 30]. Our samples also show magnetoelectric phase separation as discussed in the two-channel transport model in this paper.

M versus H curves at room temperature and M versus T curves under 5 T applied magnetic field for IFCO and ISFCO samples are shown in figure 2. It can be seen from figures 2(a) and (b) that all samples show clear ferromagnetic behavior, including the Cu-undoped samples. Room temperature FM in the Fe-doped In_2O_3 sample without Cu co-doping was also observed by Jayakumar *et al* [17], whereas it was not observed by He *et al* [14]. From the M–H curves one can clearly see the paramagnetic contribution from magnetic ions evidenced by the nonsaturation magnetization at high field. Saturation magnetization M_S obtained from the $M(H)$

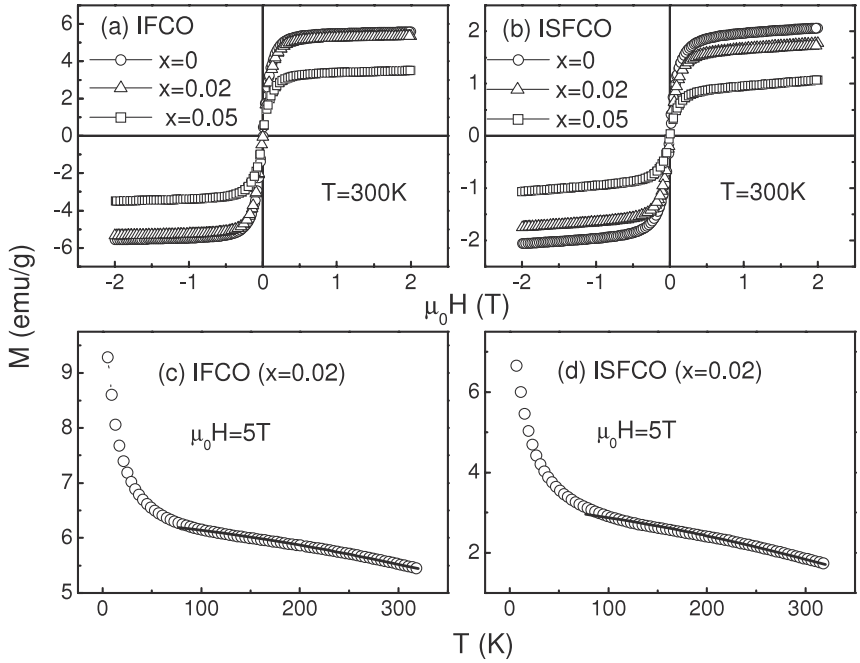

Figure 2. (a), (b) The magnetic field dependence of the magnetization for IFCO and ISFCO bulk samples. (c), (d) The temperature dependence of the magnetization for $(In_{0.83}Fe_{0.15}Cu_{0.02})_2O_3$ and $(In_{0.78}Sn_{0.05}Fe_{0.15}Cu_{0.02})_2O_3$ in a high field of 5 T. The solid lines in (c) and (d) are the fitting results according to the Block's law for spin waves.

data at 300 and 5 K is listed in table 1 after subtracting the paramagnetic component. As can be seen from the table, the sample without Cu co-doping showed a maximum M_S in both IFCO and ISFCO series and the M_S decreases monotonically with increasing Cu-doping level. The result is different from that observed in the Cu and Fe co-doped ZnO system, where M_S increases with increasing Cu doping [20]. From the large M_S value of $(In_{0.82}Fe_{0.15}Cu_{0.02})_2O_3$ (0.868 μ_B/Fe), we can conclude that the ferromagnetism is not due to impurity Fe_3O_4 and $CuFe_2O_4$. Based on our XRD results, we can suppose that at most 1% Fe will form Fe_3O_4 or $CuFe_2O_4$ impurities for the total 15% Fe doping. If all the magnetization originates from the impurities, the M_S value of the Fe_3O_4 or $CuFe_2O_4$ will be about $0.868 \times 15 = 13$ μ_B/Fe, which is an unreasonable result. Therefore, the large saturation magnetization indicates that the ferromagnetism mainly comes from the Fe in the bixbyite structure. It is also worth noting that M_S can decrease by more than 58% with 5% Sn doping, which is further evidence that the impurity induced ferromagnetism is not important for the present samples, because the XRD results as aforementioned and resistance measurements as shown later indicate that Sn does dissolve into the bixbyite In_2O_3 structure. As discussed in previous literature [15], due to the random distribution of the 15% doped Fe (chemically homogeneous), both AFM and FM interactions exist in the present samples (magnetically inhomogeneous). The decrease of the M_S value with increasing Cu and Sn concentration in the present samples can be attributed to the change of AFM and FM interactions, which may originate from the carrier density change due to Cu and Sn doping or the mediated effect of Cu and Sn in Fe–Fe interactions.

The M versus T curve under high magnetic field $\mu_0 H = 5$ T for $(In_{0.83}Fe_{0.15}Cu_{0.02})_2O_3$ and $(In_{0.78}Sn_{0.05}Fe_{0.15}Cu_{0.02})_2O_3$ is shown in figures 2(c) and (d) respectively. The steep increase with decreasing temperatures below about 50 K in the magnetization is characteristic of many DMS materials, and is probably related to the paramagnetic contribution from the doped magnetic ions. From the curve shape of M versus T above 100 K, it is clear that the material is not superparamagnetic, for which M is proportional to $1/(T - \theta)$ where θ is the blocking temperature, therefore the superparamagnetism due to small Fe_3O_4 and $CuFe_2O_4$ impurities is ruled out. The other possible origins for the ferromagnetic behavior are the intrinsic ferromagnetism due to interactions between Fe in the cubic bixbyite structure and the ferromagnetism originating from large Fe_3O_4, Fe_2O_3 and $CuFe_2O_4$ impurities which are not single domain superparamagnets. The intrinsic ferromagnetic behavior should show disordered or amorphous ferromagnetic characteristics because of the random distribution of Fe in the bixbyite structure, while the impurities are crystalline ferromagnets. One of the difference of a disordered ferromagnet and crystalline ferromagnet is the spin wave stiffness [17], which can be determined by the Bloch law fitting $M_S(T) = M_S(0)(1 - BT^{3/2})$, where B is a parameter inversely proportional to the spin wave stiffness. Our fitting shows that all the B values of the six samples are about 10^{-5} $K^{-3/2}$, which is a typical value for disordered and amorphous ferromagnets. If the ferromagnetism is due to the crystalline ferromagnetic impurity, the order of magnitude of B should be one order smaller because of the higher value of the spin wave stiffness. Therefore the impurity induced ferromagnetism

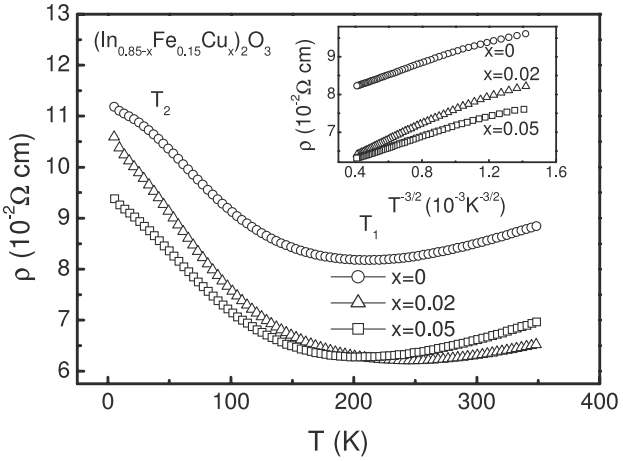

Figure 3. The temperature dependence of the resistivity of IFCO samples at zero field. The inset shows the ρ versus $T^{-3/2}$ plot.

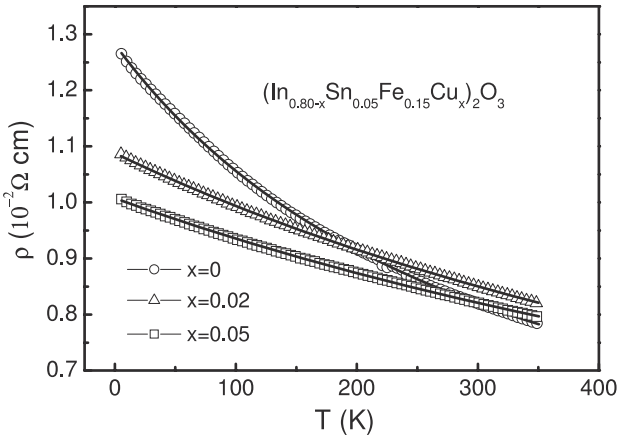

Figure 4. Resistivity versus temperature for ISFCO samples at zero field. The solid lines are the fitting curves based on the FIT model.

is ruled out, which is consistent with the results obtained from HRTEM, XAS, XANES, EXAFS, and similar curve fitting in recent literature [14, 17, 19]. The fitting curves for $(In_{0.83}Fe_{0.15}Cu_{0.02})_2O_3$ and $(In_{0.78}Sn_{0.05}Fe_{0.15}Cu_{0.02})_2O_3$ are shown in figures 2(c) and (d) respectively. The good fitting even at room temperature indicates that the Curie temperature of the amorphous or disordered ferromagnetism is far above room temperature.

The temperature dependences of the resistivity $\rho(T)$ for IFCO and ISFCO samples are shown in figures 3 and 4 respectively. It can be clearly seen that the two series of samples display different $\rho(T)$ behavior. There is a minimum in the $\rho(T)$ curve near $T_1 \sim 200$ K for bulk IFCO samples. When $T > T_1$ the temperature coefficient of resistivity is positive, while for $T < T_1$ it is negative. A similar crossover from metallic to semiconducting transport behavior is also observed in ITO nanoparticle thin film, Cr-doped In_2O_3, and Ni-doped ITO bulk samples [21–23]. The transition temperatures T_1 in IFCO are 210.7, 244.7, and 207.2 K for the samples with $x = 0$, 0.02, and 0.05 respectively. In addition to the transition at T_1, there also exists another resistivity anomaly near $T_2 \sim 30$ K. The origin of the anomaly is not clear at present. As for the $\rho(T)$ curves for ISFCO samples, only semiconducting behavior can be observed in the whole studied temperature range. ρ increases smoothly with decreasing temperature from 350 to 5 K. As shown in table 2, the low temperature resistivity at 5 K decreases monotonically with increasing Cu-doping concentration in both IFCO and ISFCO samples. The resistivity at 5 K of ISFCO samples is about one order of magnitude smaller compared to the respective IFCO samples. The resistivity decrease with Cu or Sn concentration is related to the increasing electron concentration as indicated by the Hall measurements discussed later.

Data fitting based on various electrical transport models was employed to understand the possible transport mechanisms for the negative temperature coefficient of resistivity in IFCO and ISFCO. The solid lines in figure 4 show the fitting results using the fluctuation induced tunneling (FIT) model [21] for IFSCO samples. In a FIT mechanism dominated system, the

Table 2. Data for the low temperature resistivity at 5 K and the fitting parameters T_0, T_1, and T_2 in the fluctuation induced tunneling model.

	x	$\rho_{5\,K}$ (Ω cm)	T_0 (K)	T_1 (K)	T_1^2/T_0 (K)
IFCO	0	0.112	—	—	—
	0.02	0.106	—	—	—
	0.05	0.094	—	—	—
ISFCO	0	0.013	567	732	945
	0.02	0.011	1883	3378	6059
	0.05	0.010	2275	3999	7029

temperature dependence of the resistivity is given by $\rho(T) = B_3 \exp(\frac{T_1}{T+T_0})$, where B_3 is a constant and T_1^2/T_0 reflects the barrier height and area between the metallic clusters in the sample. Good agreement between the experimental and fitting curves can be obtained in the whole studied temperature range, which suggests that the resistivity in ISFCO is dominated by the fluctuation induced tunneling between metallic regions. The fitting parameters T_0 and T_1 along with $T_1^2/T_0 = aSV^{5/2}$ are listed in table 2, where a, S and V are a constant, barrier area and barrier height respectively. The coefficient T_1^2/T_0 increases monotonically with increasing Cu-doping content, indicating the increasing barrier heights or barrier area in these ISFCO bulk samples. This interesting result shows that the Cu rich region is the barrier region in ISFCO, although the Cu doping can decrease the resistivity in both IFCO and ISFCO.

We also tried to fit the low temperature resistivity data below 200 K for IFCO samples. The inset of figure 3 presents data for IFCO plotted as $\rho(T)$ versus $T^{-3/2}$ in the temperature range of 80–200 K. The almost linear dependence shows that the scattering of conduction electrons by ionized impurities governs the temperature dependent transport properties in a limited temperature range in present samples. The obtained result is consistent with that speculated by Ederth *et al* [21]. When the temperature decreases further from 80 K, no existing models can describe the resistivity data very well.

The temperature dependence of the resistivity for all samples is also measured under an applied magnetic field of 2 T. For the ISFCO samples, no obvious MR effect was

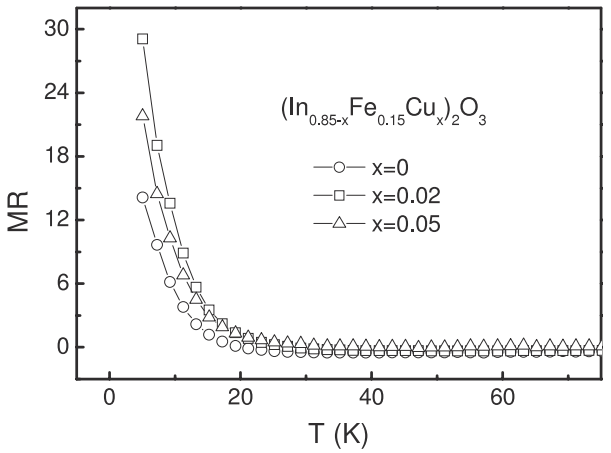

Figure 5. Magnetoresistance as a function of temperature for IFCO samples under applied field of $\mu_0 H = 2$ T.

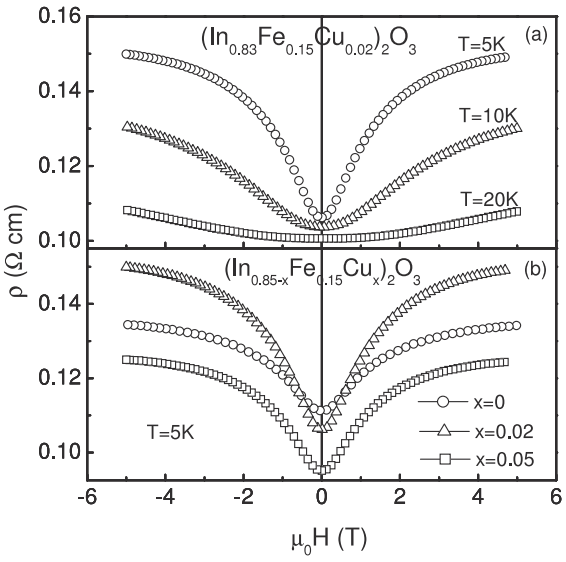

Figure 6. (a) Isothermal MR at 5, 10, and 20 K for the $(In_{0.83}Fe_{0.15}Cu_{0.02})_2O_3$ sample. (b) Isothermal MR at 5 K for $(In_{0.85-x}Fe_{0.15}Cu_x)_2O_3$ samples with $x = 0$, 0.02, and 0.05.

observed in the whole temperature range. In contrast, all the IFCO samples show interesting temperature dependent MR (defined as MR $= [R(H) - R(0)]/R(0)$) effects. As shown in figure 5, positive MR appears at low temperatures. The MR value decreases drastically with increasing temperature and changes to a negative value when $T > 30$ K. The very different magnetoresistance behavior in ISFCO and IFCO may indicate that there are two transport channels in ISFCO. The low resistance channel is formed by the Sn rich region. For the electrons in the Sn rich region, the Fe and Cu rich region is the energy barrier region. The barrier height and area will increase with increasing Cu-doping level, which is shown by the T_1^2/T_0 increase in the FIT electrical transport model with increasing Cu doping as mentioned. The higher resistance channel is for the electron transport in the Fe and Cu rich area. Most of the electrons flow in the Sn rich region, which may be a nonmagnetic region, therefore ISFCO samples do not show any MR effect. In IFCO samples, the resistance in the Fe and Cu rich region is not much higher or even lower than that of other parts of the sample. Many of the conducting electrons can pass through the ferromagnetic region (Fe and Cu rich) and show the MR effect.

In order to elucidate the origin of the positive MR features for IFCO samples, the field dependent resistivity at 5 K is also measured and the result is shown in figure 6(b). All IFCO samples show large positive MR at 5 K. The MR for the $x = 0.02$ sample at high magnetic field up to 8.5 T shows a weak resistivity peak near 8 T (not shown here). Similar MR behavior, namely, large positive MR at low field and weak negative MR at high field, was also observed in the transition-metal-doped ZnO thin films [24]. However, the magnetic field at the MR peak in the present samples is much larger than that in the doped ZnO films. In general, the weak negative MR at high field is considered to originate from the decrease of spin-disorder scattering of electrons by isolated doped magnetic ions or linked to bound magnetic polaron formation, which is still not clearly understood at present. Although the low temperature resistivity decreases monotonically with increasing Cu-doping content, the MR value at 5 K for $(In_{0.85-x}Fe_{0.15}Cu_x)_2O_3$ samples shows a complicated behavior, which increases initially with increasing Cu-doping content and then decreases. The largest MR value of 40.5% at 5 K and 5 T magnetic field is obtained for the $x = 0.02$ sample. To study the thermal effect on the MR behavior, we also measured the field dependence of the resistivity for these samples at 5, 10, and 20 K and the result for the 0.02 sample is plotted in figure 6(a). As can be seen from the figure, the positive MR in $(In_{0.83}Fe_{0.15}Cu_{0.02})_2O_3$ strongly depends on the temperature. It decreases drastically with increasing temperature from 40.5% at $T = 5$ K to 6.4% at $T = 20$ K at 5 T magnetic field. When the temperature is higher than 30 K, negative MR appears. Positive MR at low temperatures in transition-metal-doped oxides is normally attributed to the spin-split conduction band caused by the stronger s–d exchange interactions between the s-band conduction electrons and the d-band electrons from the doped ions [25–27]. The drastic decrease of the positive MR with increasing temperature in the IFCO samples shows the fast decrease of the s–d exchange interactions.

Hall resistivity ρ_{xy} at 5 K and 300 K was measured for IFCO and ISFCO samples respectively. Figure 7 shows the magnetic field dependent anomalous Hall resistivity ρ_{xy} for IFCO samples at 5 K and 300 K respectively. No AHE was found in IFSCO samples. All data in the figure were obtained by a simple subtraction $\rho_{xy} = \frac{1}{2}[\rho_{xy}(H^+) - \rho_{xy}(H^-)]$ to eliminate the MR effect. Both IFCO and ISFCO samples show n-type electron transport. The electron densities for all samples are listed in table 1. As expected, the electron density in ISFCO is almost one order larger than that in IFCO. Except for the $x = 0$ sample in IFCO, the number of carriers at both 5 and 300 K increases monotonically with increasing Cu-doping content. The evolution of n with Cu content here is contrary to that in Cu and Fe co-doped ZnO bulk samples [20]. XPS measurements show that the valence state of Cu in the doped ZnO is Cu^{1+}, rather than Cu^{2+}. Cu ions there were considered to play the role of acceptors and reduce the number of electron

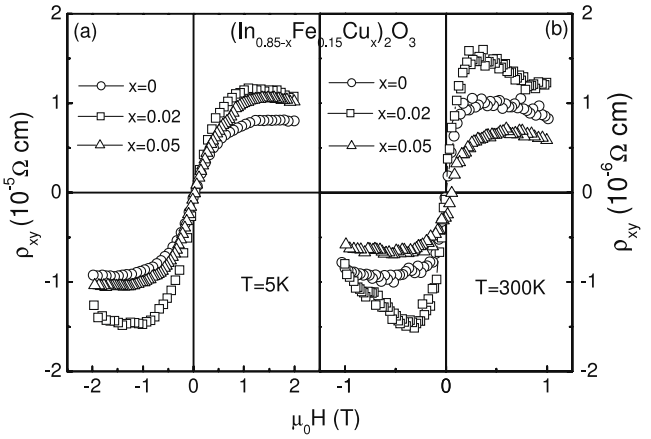

Figure 7. Anomalous Hall effect after subtracting the ordinary Hall effect term for IFCO samples. The data were collected at (a) 5 K and (b) 300 K.

carriers. Following this consideration, the valence state of Cu in the present sample is suggested to be Cu^{3+}, and Cu ions can play the role of donors and increase the electron concentration.

IFCO samples show AHE while no sign of AHE appears for ISFCO samples. This phenomenon can also be clarified by the two-channel transport model as mentioned previously. In ISFCO samples most electrons transporting in the Sn rich region are not spin polarized and therefore show no AHE, while for IFCO samples the electron transport in the ferromagnetic Fe and Cu rich region will be spin polarized and show AHE. The magnitude of the AHE (here defined by $\rho_{xy}^{\mathrm{AHE}}/\rho_{xx} \sim 10^{-4}$) is much smaller than that of (Ga, Mn)As ($\rho_{xy}^{\mathrm{AHE}}/\rho_{xx} \sim 10^{-2}$) [28], which may indicate that there are many electrons transporting in the nonmagnetic region even in IFCO samples. To make a useful material for spintronics application, we should increase the ferromagnetic area or increase the resistance of the nonferromagnetic region. Further research work will be performed in this direction.

4. Conclusions

In conclusion, bulk polycrystalline samples of $(In_{0.85-x}Fe_{0.15}Cu_x)_2O_3$ and $(In_{0.80-x}Sn_{0.05}Fe_{0.15}Cu_x)_2O_3$ have been synthesized by the solid state reaction method in vacuum conditions. All samples show clear room temperature FM and the saturated magnetic moment decreases monotonically with increasing Cu-doping level. The analysis based on the magnetic measurement results indicates that the ferromagnetism is not due to the impurity Fe_3O_4 and $CuFe_2O_4$. A crossover from semiconducting behavior to metallic behavior with increasing temperature in the $\rho(T)$ curve is observed in the IFCO samples, whereas only semiconducting behavior can be observed in ISFCO samples. The semiconducting resistivity of ISFCO is dominated by the fluctuation induced tunneling mechanism. For IFCO, the temperature dependent resistivity is governed by ionized impurity scattering in a limited temperature range. Both positive MR and AHE are observed at low temperatures in IFCO, but not in ISFCO compounds. All the electric transport measurement results can be clarified by a two-channel transport model.

Acknowledgments

This work was supported by research grant RG5906 funded by the Singapore Ministry of Education Academic Research Fund Tier 1 and A*star SERC grant 062 101 00300.

References

[1] Wolf S A, Awschalom D D, Buhrman R A, Daughton J M, von Molnar S, Roukes M L, Chtchelkanova A Y and Treger D M 2001 *Science* **294** 1488
[2] Dietl T, Ohno H, Matsukura F, Cibert J and Ferrand D 2000 *Science* **287** 1019
[3] Ueda K, Tabata H and Kawai T 2001 *Appl. Phys. Lett.* **79** 988
[4] Sluiter M H F, Kawazoe Y, Sharma P, Inoue A, Raju A R, Rout C and Waghmare U V 2005 *Phys. Rev. Lett.* **94** 187204
[5] Wang Z, Tang J, Tung L D, Zhou W and Spinu L 2003 *J. Appl. Phys.* **93** 7870
[6] Hong N H, Sakai J, Prellier W, Hassini A, Ruyter A and Gervais F 2004 *Phys. Rev.* B **70** 195204
[7] Ogale S B *et al* 2003 *Phys. Rev. Lett.* **91** 077205
[8] Coey J M D, Douvalis A P, Fitzgerald C B and Venkatesan M 2004 *Appl. Phys. Lett.* **84** 1332
[9] Fukumura T, Toyosaki H and Yamada Y 2005 *Semicond. Sci. Technol.* **20** S103
[10] Neal J R, Behan A J, Ibrahim R M, Blythe H J, Ziese M, Fox A M and Gehring G A 2006 *Phys. Rev. Lett.* **96** 197208
[11] Rao C N R and Deepak F L 2005 *J. Mater. Chem.* **15** 573
[12] Bérardan D and Guilmeau E 2007 *J. Phys.: Condens. Matter* **19** 236224
[13] Pearton S J, Abernathy C R, Overberg M E, Thaler G T, Norton D P, Theodoropoulou N, Hebard A F and Park Y D 2003 *J. Appl. Phys.* **93** 1
[14] He J, Xu S F, Yoo Y K, Xue Q, Lee H C, Cheng S, Xiang X-D, Dionne G and Takeuchi I 2005 *Appl. Phys. Lett.* **86** 052503
[15] Yoo Y K *et al* 2005 *Appl. Phys. Lett.* **86** 042506
[16] Kohiki S *et al* 2006 *Thin Solid Films* **505** 122
[17] Jayakumar O D *et al* 2007 *Appl. Phys. Lett.* **91** 052504
[18] Ohno T, Kawahara T, Tanaka H, Kawai T, Oku M, Okada K and Kohiki S 2006 *Japan. J. Appl. Phys.* **36** L957
[19] Yu Z G, He J, Xu S F, Xue Q Z, van't Erve O M J, Jonker B T, Marcus M A, Yoo Y K, Cheng S F and Xiang X D 2006 *Phys. Rev.* B **74** 165321
[20] Han S-J, Song J W, Yang C-H, Park S H, Park J-H, Jeong Y H and Rhie K W 2002 *Appl. Phys. Lett.* **81** 4212
[21] Ederth J, Johnsson P, Niklasson G A, Hoel A, Hultaker A, Heszler P, Granqvist C G, van Doorn A R, Jongerius M J and Burgard D 2003 *Phys. Rev.* B **68** 155410
[22] Kharel P, Sudakar C, Sahana M B, Lawes G, Suryanarayanan R, Naik R and Naik V M 2007 *J. Appl. Phys.* **101** 09H117
[23] Peleckis G, Wang X L and Dou S X 2006 *Appl. Phys. Lett.* **89** 022501
[24] Dietl T, Andrearczyk T, Lipińska A, Kiecana M, Tay M and Wu Y H 2007 *Phys. Rev.* B **76** 155312
[25] Fukumura T, Jin Z, Ohtomo A, Koinuma H and Kawasaki M 1999 *Appl. Phys. Lett.* **75** 3366
[26] Andrearczyk T, Jaroszyński J, Grabecki G, Dietl T, Fukumura T and Kawasaki M 2005 *Phys. Rev.* B **72** 121309
[27] Kim J H, Kim H, Kim D, Ihm Y E and Choo W K 2003 *Physica* B **327** 304
[28] Matsukura F, Ohno H, Shen A and Sugawara Y 1998 *Phys. Rev.* B **57** R2037
[29] Kuhns P L, Hoch M J R, Moulton W G, Reyes A P, Wu J and Leighton C 2003 *Phys. Rev. Lett.* **91** 127202
[30] Dagotto E, Hotta T and Moreo A 2001 *Phys. Rep.* **344** 1